

Conformational changes in the expression domain of the *Escherichia coli* thiM riboswitch

Andrea Rentmeister, Günter Mayer, Nicole Kuhn and Michael Famulok*

LIMES Program Unit Chemical Biology & Medicinal Chemistry, Kekulé Institute for Organic Chemistry & Biochemistry, University of Bonn, Gerhard-Domagk-Strasse 1, D-53121 Bonn, Germany

Received January 24, 2007; Revised and Accepted April 14, 2007

ABSTRACT

The thiM riboswitch contains an aptamer domain that adaptively binds the coenzyme thiamine pyrophosphate (TPP). The binding of TPP to the aptamer domain induces structural rearrangements that are relayed to a second domain, the so-called expression domain, thereby interfering with gene expression. The recently solved crystal structures of the aptamer domains of the thiM riboswitches in complex with TPP revealed how TPP stabilizes secondary and tertiary structures in the RNA ligand complex. To understand the global modes of reorganization between the two domains upon metabolite binding the structure of the entire riboswitch in presence and absence of TPP needs to be determined. Here we report the secondary structure of the entire thiM riboswitch from *Escherichia coli* in its TPP-free form and its transition into the TPP-bound variant, thereby depicting domains of the riboswitch that serve as communication links between the aptamer and the expression domain. Furthermore, structural probing provides an explanation for the lack of genetic control exerted by a riboswitch variant with mutations in the expression domain that still binds TPP.

INTRODUCTION

Riboswitches are conserved non-coding elements located in the untranslated regions of mRNAs that regulate the expression of genes in biosynthetic pathways in response to metabolite binding (1,2). Thiamine pyrophosphate (TPP)-sensing riboswitches control genes involved in the biosynthesis and transport of the coenzyme thiamine (3). The thiM riboswitch from *Escherichia coli* is a genetic element that regulates the expression of the enzyme hydroxyethylthiazol kinase (4). The riboswitch exhibits

strong TPP-binding activity and the structure of the aptamer domain of the riboswitch in complex with TPP has recently been solved (5,6). The gene expression domain of the *E. coli* thiM riboswitch comprises a five-nucleotide motif that likely serves as a ribosomal recognition site as it shows homology to the Shine–Dalgarno sequence (SD). Gene regulation presumably occurs at the level of translational initiation and is assumed to depend mostly on the accessibility of the SD sequence. In the absence of TPP the SD sequence is thought to be accessible for the ribosome, whereas TPP-binding to the aptamer domain of the riboswitch at concentrations above a certain threshold induces structural reorganizations that finally result in sequestration of the SD-sequence, rendering it inaccessible for the ribosome. Although the X-ray structures of the aptamer domains reveal insights into the complex-formation of the thiM riboswitch, the conformational changes that are exerted in the expression domain remain unknown (7–10). This issue can be addressed by crystallization studies of the full-length riboswitch in the presence and absence of TPP. However, only one full-length riboswitch, the S-adenosylmethionine (SAM) binding riboswitch from *Thermoanaerobacter tengcongensis*, was solved in its metabolite-bound state (11). This structure impressively revealed that parts of the riboswitch serve as a communication link between the aptamer and the expression-domain. Upon metabolite binding this module facilitates the transduction of conformational changes from the aptamer- to the expression-domain that are induced by SAM. We applied an alternative approach which makes use of short RNA hairpins that recognize the TPP-free conformation of the thiM riboswitch (12). One RNA hairpin was shown to bind tightly to the expression-domain and mutational and functional analyses revealed that the binding site of the hairpin is important for the proper function of the thiM riboswitch in *E. coli*. Based on these findings, we now report the secondary structure of the full-length thiM riboswitch in its TPP-free form and the conformational changes observed upon the addition of TPP. Furthermore, we analyzed a previously

*To whom correspondence should be addressed. Tel: +49-228-735661; Fax: +49-228-735388; Email: m.famulok@uni-bonn.de

The authors wish it to be known that, in their opinion, the first two authors should be regarded as joint First Authors

© 2007 The Author(s)

This is an Open Access article distributed under the terms of the Creative Commons Attribution Non-Commercial License (<http://creativecommons.org/licenses/by-nc/2.0/uk/>) which permits unrestricted non-commercial use, distribution, and reproduction in any medium, provided the original work is properly cited.

described expression domain mutant of the thiM riboswitch that still binds to TPP but does not exert genetic control.

MATERIALS AND METHODS

Enzymatic probing of RNA secondary structures

Enzymatic probing was performed as described previously (20). Specifically, after removal of 5'-triphosphate with CIAP (calf intestine alkaline phosphatase, Stratagene) RNAs were 5'-end-labeled with [γ - 32 P]ATP using T4 PNK (New England Biolabs) and PAGE purified. Traces of labeled RNA were incubated with RNase S (Promega), V1, A or T1 (Ambion), either in the presence or absence of TPP in cleavage buffer (10 mM Tris pH 7.5, 100 mM KCl and 5 mM MgCl₂, 1 μ g tRNA). Prior to the addition of nucleases, RNA was denatured by incubation at 95°C for 5 min and allowed to fold by slowly cooling to room temperature for 40 min in the presence of MgCl₂ and TPP (Sigma) if indicated. Subsequently, the reactions were precipitated, dissolved in PAGE-loading buffer and analyzed on a 10% denaturing PAA-gel. RNA markers were prepared by partial digestion with alkaline solution and cleavage with RNase T1 under denaturing conditions. Visualization was done by PhosphorImaging (Fuji, FLA3000).

Filter-binding assays

Biotinylated thiM RNA (35 nM) was incubated with [32 P]-end labeled RNA hairpin N25.1.22 (1 nM), 35 nM soluble streptavidin, and varying concentrations of MgCl₂ in binding buffer (10 mM HEPES pH 7.5, 100 mM KCl) for 30 min at RT. After incubation, the reactions were passed through 0.45 μ m nitrocellulose membranes and washed four times with 200 μ l binding buffer. Bound RNA was quantified by PhosphorImaging. All assays were performed in quadruplicates.

Chemical probing of RNA secondary structures

Chemical probing was performed as described previously (20). Modification with DMS or kethoxal: In a final volume of 10 μ l, RNA (0.2 μ g/ μ l) was incubated in 50 mM HEPES pH 7.8, 100 mM KCl, 10 mM MgCl₂ with 0–4.5 mM TPP (Sigma) at 25°C for 30 min. Then, 1 μ l of a 600 mM solution of DMS in ethanol or 200 mM kethoxal (ICN) in water, respectively was added, mixed and incubated 20 min at 25°C. After precipitation, 5'-end labeled primer was annealed and primer extension performed. Modification with CMCT: In a final volume of 10 μ l, RNA (0.2 μ g/ μ l) was incubated in 50 mM potassium borate pH 8.0, 100 mM KCl, 10 mM MgCl₂ with 0–4.5 mM TPP (Sigma) at 25°C for 30 min. Then 1 μ l of a 200 mM solution of CMCT in water was added, mixed and incubated 20 min at 25°C. After precipitation, 5'-end labeled primer was annealed and primer extension performed. In a 20 μ l reaction 0.2 μ g RNA in 50 mM Tris-HCl (pH 8.3), 75 mM KCl, 3 mM MgCl₂, 20 mM DTT, 0.5 mM dNTPs (each) was heated to 65°C for 5 min, then chilled on ice for 1 min. After addition of 1 μ l (200U)

of Superscript II Reverse Transcriptase (Invitrogen) the reaction was incubated at 42°C for 50 min, followed by inactivation at 70°C for 15 min. After precipitation the DNA fragments were separated on an 8% denaturing PAA gel at 2000 V and visualized by PhosphorImaging. The sequencing reactions were carried out using the PCR templates with the Sequenase Version 2.0 PCR Product Sequencing kit (USB). To monitor TPP-induced changes of the chemical modifications of 165 thiM we used *in situ* probing. For this purpose, the respective DNA templates were *in vitro* transcribed in the respective probing buffer (50 mM HEPES pH 7.8, 100 mM KCl, 15 mM MgCl₂ for DMS and kethoxal probing; 50 mM potassium borate pH 8.0, 100 mM KCl, 15 mM MgCl₂ for CMCT probing) in the presence of 0–3 mM TPP for 3 h and used directly for chemical probing. The amount of RNA in the reactions was equal, as determined on 2.5% agarose-gels.

Preparation of oligonucleotides

ThiM riboswitches were prepared from dsDNA templates, generated by PCR using the appropriate primers, by *in vitro* transcription and purified by PAGE. 5'-biotinylated RNA was prepared by GMPS transcription, using 4-fold excess of GMPS over GTP, and subsequent treatment with iodo-acetyl biotin (Pierce). For the preparation of the RNA hairpin N25.1.22 the complementary oligos 22.1F and 22.1R were hybridized and used for *in vitro* transcription by T7 RNA polymerase. The Mutant M4 was generated by QuickChange (Stratagene) according to the manufacturer's instructions.

RESULTS

Secondary structure of the TPP-free form of the thiM riboswitch from *E. coli*

We previously identified an RNA hairpin (N25.1.22) with a loop sequence which is complementary to nt 95–101 of the *E. coli* thiM riboswitch (12). We showed that the RNA hairpin binds to the expression domain of the thiM riboswitch, thereby specifically competing with TPP but not with thiamine for binding. This allowed the conclusion that the binding region of the hairpin to the riboswitch undergoes fundamental structural rearrangements upon metabolite binding. Figure 1A depicts the respective RNA hairpin N25.1.22 and the complementary region responsible for thiM binding highlighted in cyan. Binding of the hairpin to thiM strictly depends on the Mg²⁺-ion concentration (Figure 1B), suggesting that the region targeted by the hairpin also forms a hairpin structure, thus allowing the formation of a kissing complex. Kissing complexes can be quite stable, even in cases where only two base pairs are involved, and frequently mediate molecular recognition events between RNA molecules (13,14). In addition, secondary structure changes required for proper thiM riboswitch function should fulfill the following criteria: (i) The region of the thiM riboswitch that binds to the RNA hairpin should be single stranded in the absence of TPP and become paired upon addition of TPP. (ii) In the TPP-free form of the thiM riboswitch

the SD sequence should be accessible for ribosome binding, thus be essentially unpaired; and (iii) the nucleotides that reside downstream of the SD region should not be engaged in extensive base-pairing secondary

structure in the TPP-free form of the thiM riboswitch, to avoid loss of translation efficiency.

A secondary structure of the TPP-free thiM riboswitch that is consistent with these requirements is shown in Figures 2A and B, respectively. In this fold, the formation of the hairpin nt 92–103, harboring the binding region (nucleotides shown in cyan) of the selected RNA hairpin N25.1.22, stipulates the pairing of residues 71–86 with nt 125–108. These pairings are consistent with both chemical (Figure 2A) and enzymatic (Figure 2B) probing data (see also Supplementary Figures S2 and S3). Chemical probing with dimethylsulfate (DMS) modifies the proposed ACCA-loop (Figure 2A, nt 96–99) whereas the adjacent stem of the hairpin remains unmodified. The observed RNase S1 and RNase A cleavages at positions A96 to A99 (Figure 2B) further indicate that the target region of the RNA hairpin indeed forms the proposed loop structure. The crystal structure of the aptamer domain of the thiM riboswitch revealed that the nt 71–86 form the paired regions P5, P4 and P1 in its TPP-bound variant, whereas the nt 108–125 are assumed

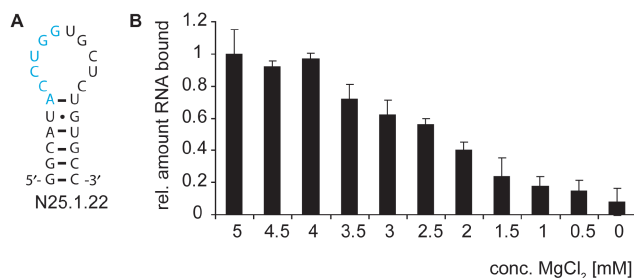


Figure 1. The *in vitro* selected hairpin N25.1.22 binds to the TPP-free form of the 165 thiM riboswitch in a Mg²⁺-dependent manner. (A) Primary sequence of the selected hairpin N25.1.22. The sequence which is complementary to the thiM riboswitch is highlighted in cyan. (B) Binding of the hairpin N25.1.22 to the thiM riboswitch is dependent on the concentration of Mg²⁺-ions in the reaction.

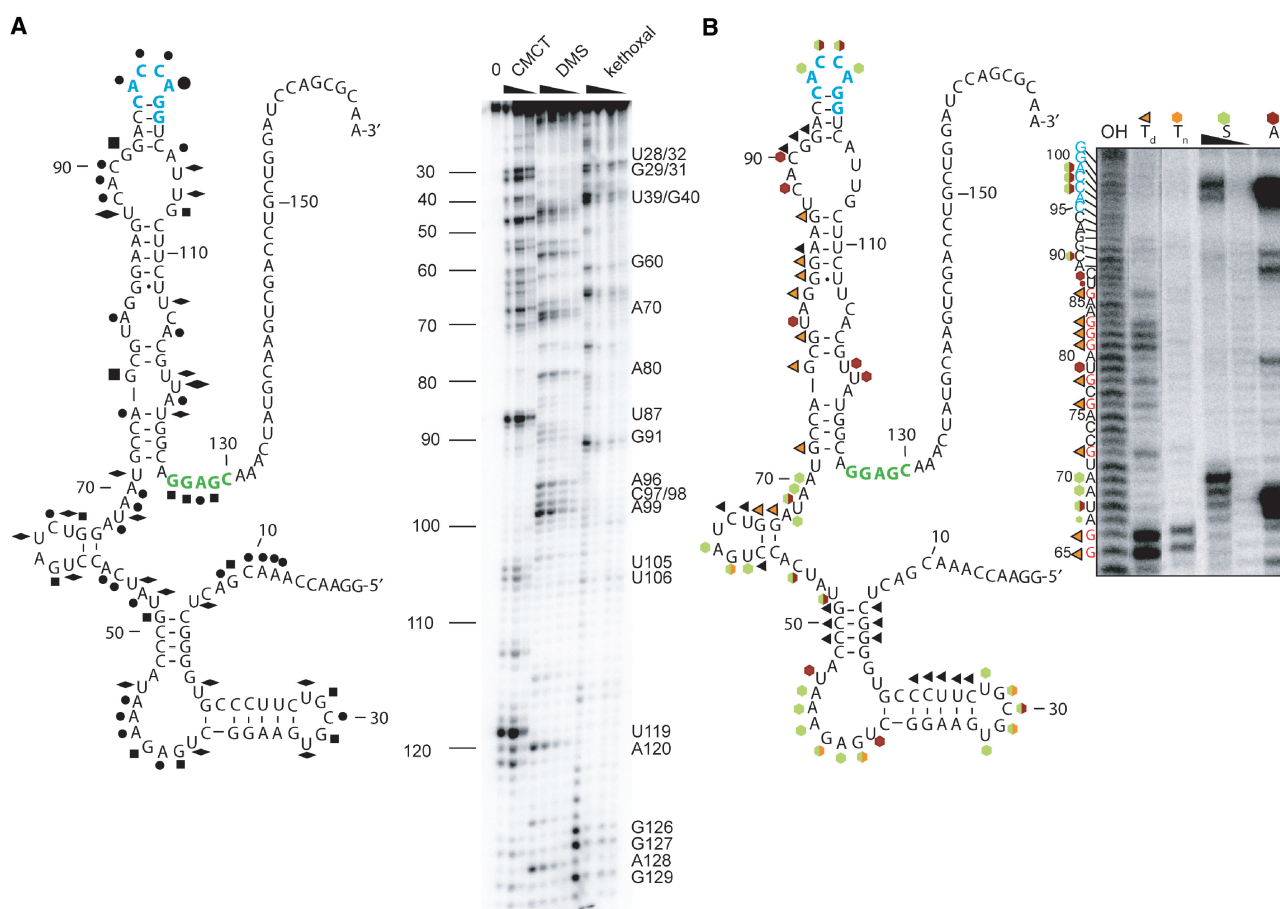


Figure 2. Proposed secondary structure of the TPP-free form of the thiM riboswitch from *E. coli*. The sequence complementary to and binding to the previously selected hairpin N25.1.22 is shown in cyan. The SD-sequence is highlighted in green. (A) Secondary structure of the TPP-free form of the thiM riboswitch (left panel) as well as primer extension reactions after chemical modifications of the riboswitch with CMCT, DMS or kethoxal (right panel). Positions that are chemically modified are marked with symbols (DMS, black dot; kethoxal, black square; CMCT, black diamond). Untreated RNA is referred to as 0. (B) Secondary structure of the TPP-free form of the thiM riboswitch (left panel) as well as enzymatic probing data (right panel) including the cleavage pattern of 5'-[³²P]-labeled 165 thiM by alkaline hydrolysis (OH) and different nuclease digestions (denaturing T1, T_d, native T1, T_n, S and A). Labels are: RNase S, green hexagons; RNase A, red hexagons; RNase T1 native, orange hexagons; RNase T1 denatured, black bordered orange triangles.

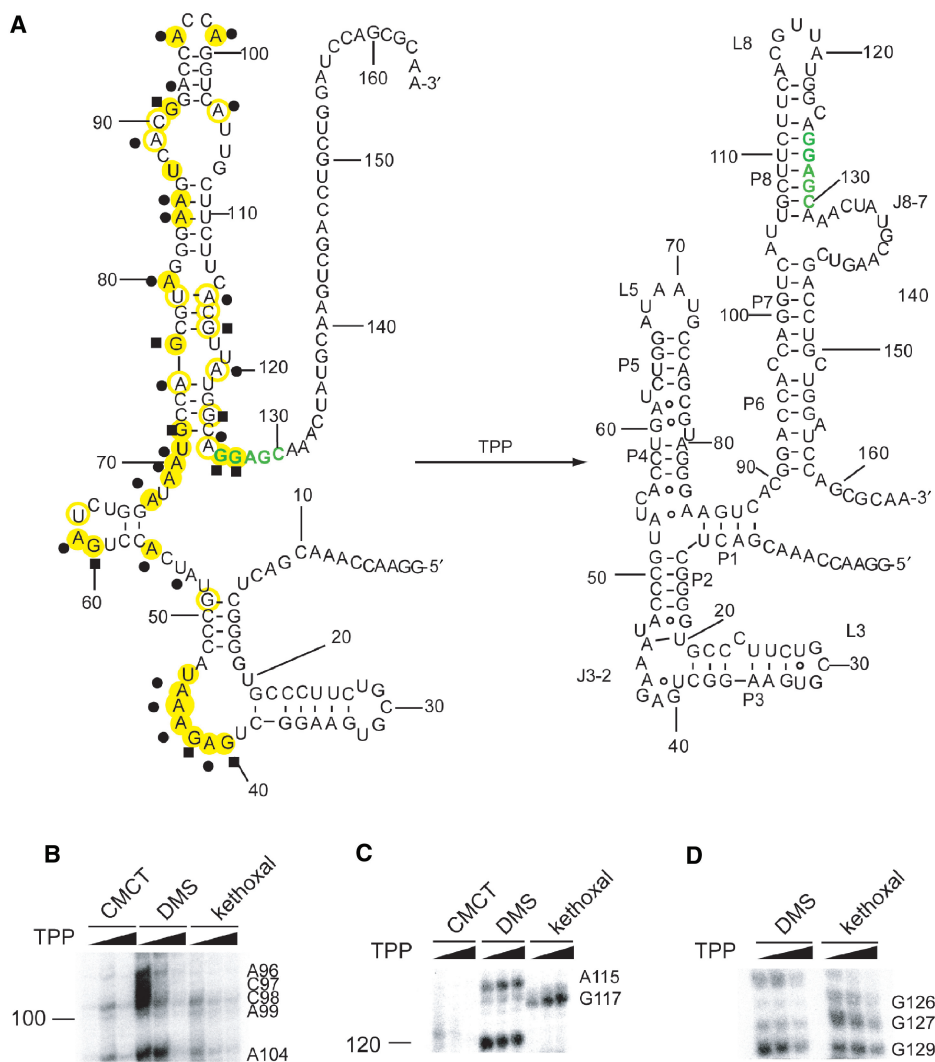


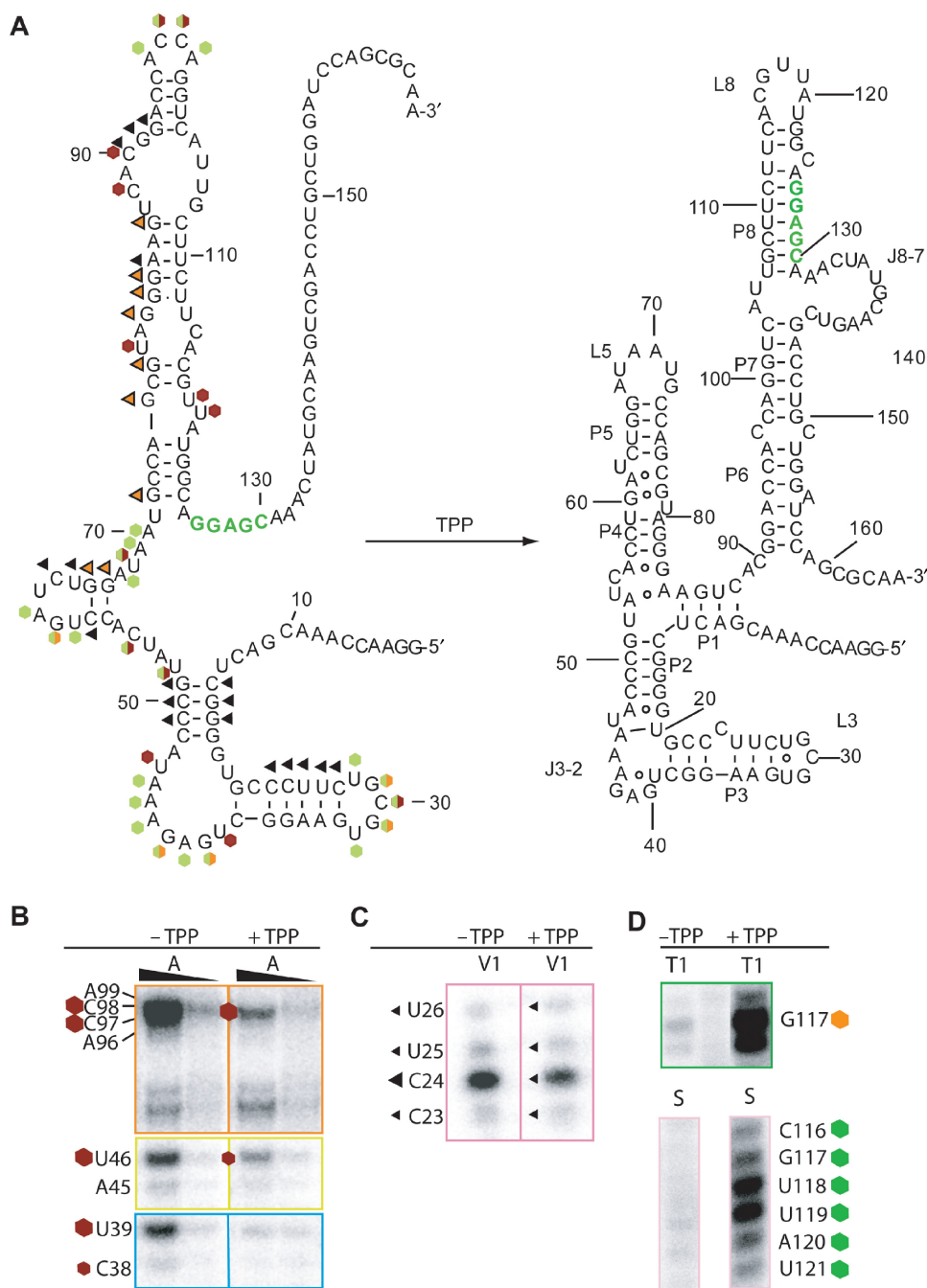
Figure 3. Chemical probing of TPP-induced structural changes in the thiM riboswitch. (A) Model of the TPP-induced structural reorganization of the thiM riboswitch. Positions that are modified in the absence of TPP are marked with symbols (DMS, black dot; kethoxal, black square; CMCT, black diamond). Positions with TPP-induced changes of the chemical modification pattern are highlighted with yellow circles (closed, decrease; open, increase in signal intensity). (B–D) Representative clippings from PAA-gels (shown in full context in Supplementary Figure S6) after chemical probing in the presence of different amounts of TPP.

to be implied in the formation of P8 and L8 of the expression domain leading to the sequestration of the SD-sequence (5). In our model of the TPP-free variant of the thiM riboswitch, the anti-SD sequence pairs with nt 83–86 in the context of an extended helix, leaving the SD-sequence unpaired and thus accessible for binding to the ribosome. These findings are supported by the chemical probing data (Figure 2A), which clearly show that nt 126–129 of the SD sequence are modified by kethoxal and DMS in the absence of TPP. Thus, in accordance with the function of the riboswitch the SD sequence is unpaired and allows initiation of translation by ribosome binding.

In our secondary structure model of the TPP-free form of the thiM riboswitch the nucleotides that are located downstream of the SD-sequence do not appear to be involved in secondary structures with upstream elements. To support this, we investigated a 3'-truncated

construct of the thiM riboswitch which completely lacks the nt 131–165. Indeed, chemical and enzymatic probing of this construct reveals that the overall folding of nt 1–130 in the absence of TPP is independent from nt 131–165 (Supplementary Figures S4C, S5).

Chemical and enzymatic probing data (Figures 3 and 4) indicate that the stems P2 and P3 of the aptamer domain are pre-organized in the absence of TPP. No modifications of the nucleotides comprising these stems were found by chemical probing and the formation of stem P2 is further supported by RNase V1 cuts that reveal that positions C15 to G17 and C49 to G51 are paired (Supplementary Figure S4B). However, chemical and enzymatic probing indicates that the positions U28 to U32 and U39 to U46 are unpaired in the absence of TPP (Figure 2A, Supplementary Figures S2, S4B). The region ranging from nt 52–70 was highly modified by chemical probing (Supplementary Figure S2B, S2C), and enzymatic



modifications of the nucleotides U39 to A43 that are essential for the recognition of the 4-amino-5-hydroxymethyl-2-methylpyrimidine (HMP) moiety of TPP are less abundant in the presence of TPP (Supplementary Figure S1). Additionally, reduced modifications of ntU28 to U32 and ntU39 to U46 in the presence of TPP were observed. This indicates that these residues become paired or involved in a more compact structure upon binding to TPP, and the data obtained by chemical probing are in agreement with the crystal structure of the complex of TPP with the aptamer domain (5,6).

Chemical probing of the 165 thiM construct revealed similar changes for nucleotides G40–U46 as well as G60 and A61 in the presence of TPP (Supplementary Figure S6C). More importantly, in chemical probing of 165 thiM in the presence of TPP, we observed changes in the expression domain of the thiM riboswitch. For example, modifications or nucleotides that are part of the SD-sequence (Figure 3D: G129 and to a lesser extent G126 and G127) were slightly decreased. This result suggests that the SD-sequence becomes involved in base pairing upon TPP binding to the aptamer domain. It is also in accordance with the proposed structural model and the generally assumed mechanism for translation inhibition by sequestration of the SD-sequence. Other TPP-induced changes can be observed within the proposed hairpin motif nt 92–103 (Figure 3B). Modifications of nucleotides A96–A99 become less intensive in the presence of TPP (Figure 3B) suggesting that this region is unpaired in the absence but becomes paired in the presence of TPP. This rearrangement results in the nearly consecutively base-paired stems P6 and P7. Notably, this conformational change explains why the RNA hairpin N25.1.22 is released from the thiM riboswitch by the addition of TPP.

The modification intensities of nucleotides U87 and A85, A84 are decreased in the presence of TPP, indicating that these nucleotides become less accessible upon binding of the metabolite (Supplementary Figure 6C). The three nucleotides U87, A85 and A84 are involved in the formation of stem P1 which resides at the connection of the aptamer- to the expression domain of the riboswitch in its TPP-bound form (Figure 3A). The adjacent nucleotide G86 however, is neither modified in the absence of TPP nor in its presence, consistent with G86 being involved in stable G–C base pairing (Supplementary Figure 6C).

The enzymatic probing experiments also indicate TPP-induced changes within the aptamer domain of the thiM riboswitch, although less pronounced as compared to the chemical probing analyses (Figure 4 and Supplementary Figure S7). The most prominent changes were observed within the helix J3-2, harboring the binding region of the HMP moiety of TPP, at nucleotides U46 and U39 (Figure 4B). The X-ray structure of the aptamer domain revealed that nucleotide C24 of stem P2 is bulged out in the presence of TPP (5). In accordance with this finding the cleavage at position C24 with RNase V1 becomes slightly protected in the presence of TPP (Figure 4C). TPP-dependent protection is

also observed for the single-strand-specific RNase A cuts at positions C38, U39 and U46 (Figure 4B), consistent with the notion that these nucleotides are essentially unpaired in absence of TPP, but form a compact structure in its presence. Enzymatic cleavages of nucleotides in the expression domain were also influenced by addition of TPP: The formation of the loop U18 becomes perceptible by RNase S1 cuts at position U118 and U119 as well as RNase T1 cleavage at G117 that are well pronounced in the presence of TPP (Figure 4D). The notion that G117 is only cleaved in the presence of TPP is consistent with G117 being embedded within a stable helical context in the TPP-free form and becoming exposed within a single-stranded loop (L8) in the TPP-bound form of thiM (Figure 4A).

TPP-induced cleavage by RNase T1 can also be detected for G123 and to a lesser extent for G122 (Supplementary Figures S7B and S7C). Positions 116–121 show strong RNase S cleavage in the presence of TPP but not in its absence (Supplementary Figure S7C). Cleavage by RNase A and S were observed at nt 96–99 which form the putative hairpin structure that is targeted by the RNA hairpin N25.1.22 (Figure 4B). Notably, these cleavages are protected in the presence of TPP, leaving only C97 accessible for the nuclease (Figure 4B). These findings are in accordance with the data that were obtained by chemical probing (Figure 3B). Taken together, they explain why the binding of the RNA hairpin N25.1.22 to the thiM riboswitch is competed by the addition of TPP. In addition, on the basis of above results, we can suggest a secondary structure model of the TPP-free form of the thiM riboswitch and its structural transition to the TPP-bound form (Figure 5). In this model, the stem regions P2 and P3 of the aptamer domain are preformed and allow the binding of the thiM riboswitch to the HMP moiety of TPP. The presence of Mg²⁺-ions complexed to pyrophosphate induces a conformational change, resulting in the formation of P4, P5 and P6–P8. Our model also explains why thiamine fails to induce the conformational changes necessary to gain genetic control, although it binds to the riboswitch, albeit with significant lower affinity.

Probing a mutant of thiM that still binds to TPP but does not exert genetic control anymore

We have previously reported a riboswitch variant containing mutations in the region nt 95–101, which is complementary to our hairpin (12). In mutant M4 the formation of stem P7 proposed for the TPP-bound riboswitch is disrupted (Figure 6A). This mutation—the substitution of G100 and G101 by two Cs—caused loss of genetic control of the corresponding β -galactosidase fusion construct although the riboswitch still bound to TPP ($K_D \sim 20$ nM) indicating that besides stem P8, which harbors the SD sequence, also the formation of stem P7 may be important for proper function of the riboswitch (12). To test whether the loss of the ability to exert genetic control in mutant M4 can be rationalized on the basis of secondary structure changes, we carried out chemical probing of this mutant. Results of chemical

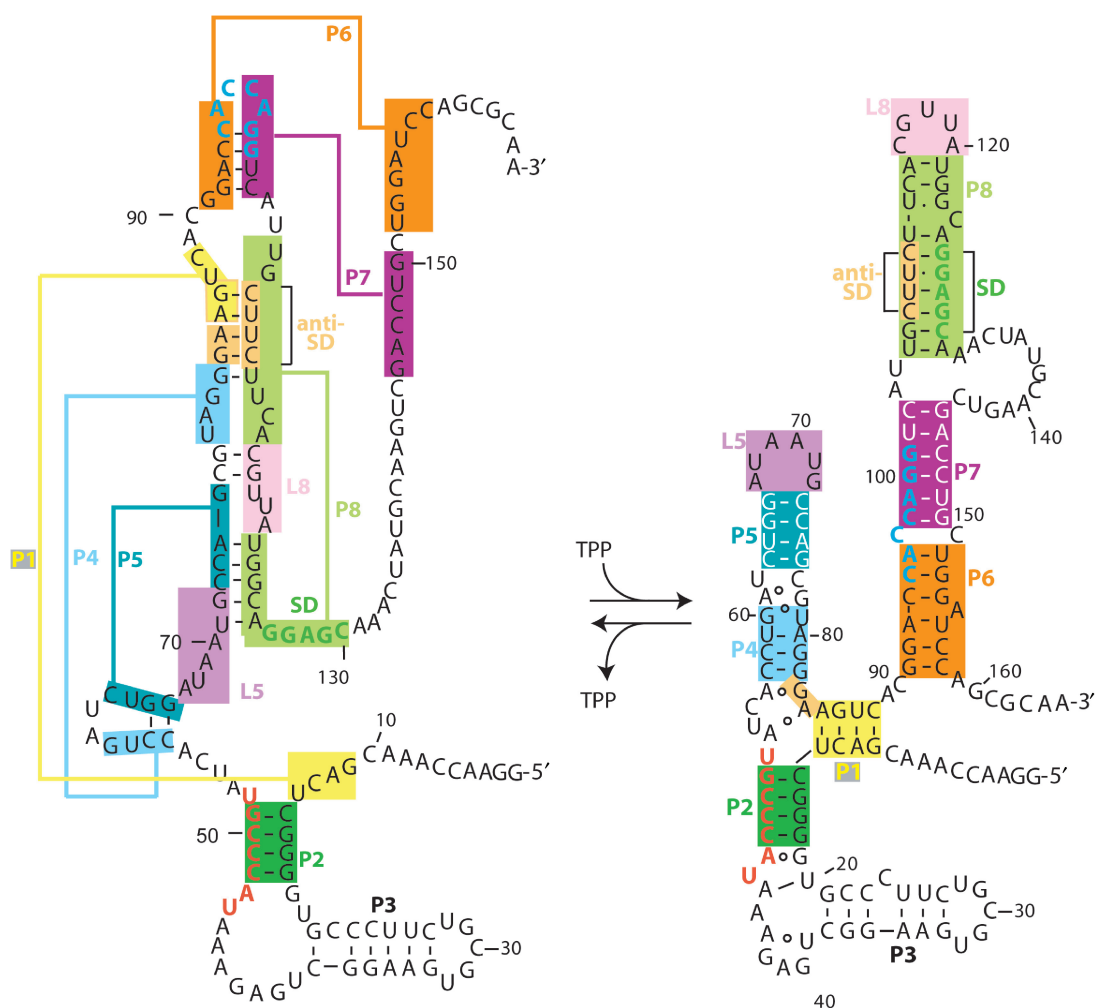


Figure 5. Intra- and inter-domain communication in the thiM riboswitch. A thiM riboswitch structure model in the absence (left) and presence (right) of TPP. Nucleotides that form stem structures or loops in the TPP-bound state are color-coded. The nucleotides representing the SD region are depicted in green and the anti-SD region is colored in light orange. Stem regions found in the TPP-bound state are numbered P1–P8 as described and the corresponding regions in the TPP-free state are connected by colored lines indicating intra- and inter-domain communication in the thiM riboswitch. The target region of the selected RNA hairpin N25.1.22 is shown in cyan. In the TPP-free state, nt 71–86 of the aptamer domain pair with the nt 108–125 of the expression domain, thus sequestering the anti-SD sequence and rendering SD free to allow translation initiation. In the TPP-free state, the target region of RNA hairpin is unpaired. Upon addition of TPP the target regions experience conformational rearrangements, resulting in base pairing of these regions.

probing as well as the derived secondary structure for M4 are shown in Figure 6 and Supplementary Figure S8. Chemical probing data for M4 in the absence of TPP are in accordance with the secondary structure resembling the TPP-bound form of the wild-type 165 thiM riboswitch (Figure 6B for nt 1–60, and lanes without TPP in Figure 6C). However, base pairing cannot be entirely maintained in stem P7 due to the introduced mutations. The aptamer domain appears to be entirely preformed also in the absence of TPP except for stem P1 (nt 85–88) that appears to be unpaired (Figure 6A and modifications in the region nt 85–88 in Figure 6C). Furthermore, the data suggest that in M4 the SD sequence is mainly paired even in the absence of TPP (absence of modifications for nt 126–130 in Figure 6C). Chemical probing in the presence of different concentrations of TPP reveals changes in the aptamer domain for nucleotides that participate either in TPP binding (e.g. U39, G40,

G60 and to a lesser extent A41, A43 in Figure 6C) or in formation of stem P1 (G86, U87 in Figure 6C). Alterations of nucleotide accessibility comprising the SD sequence were not observed.

Taken together, these data indicate that structural alterations in the expression domain of this mutant do not occur to the degree necessary for proper gene regulation upon addition of TPP, although TPP is bound by the preformed aptamer domain. The derived secondary structure is in accordance with our previously reported observations that M4 can still bind to TPP but does not exert genetic control any more.

DISCUSSION

In this study, we have elucidated the conformational changes that occur in the *E. coli* thiM riboswitch during

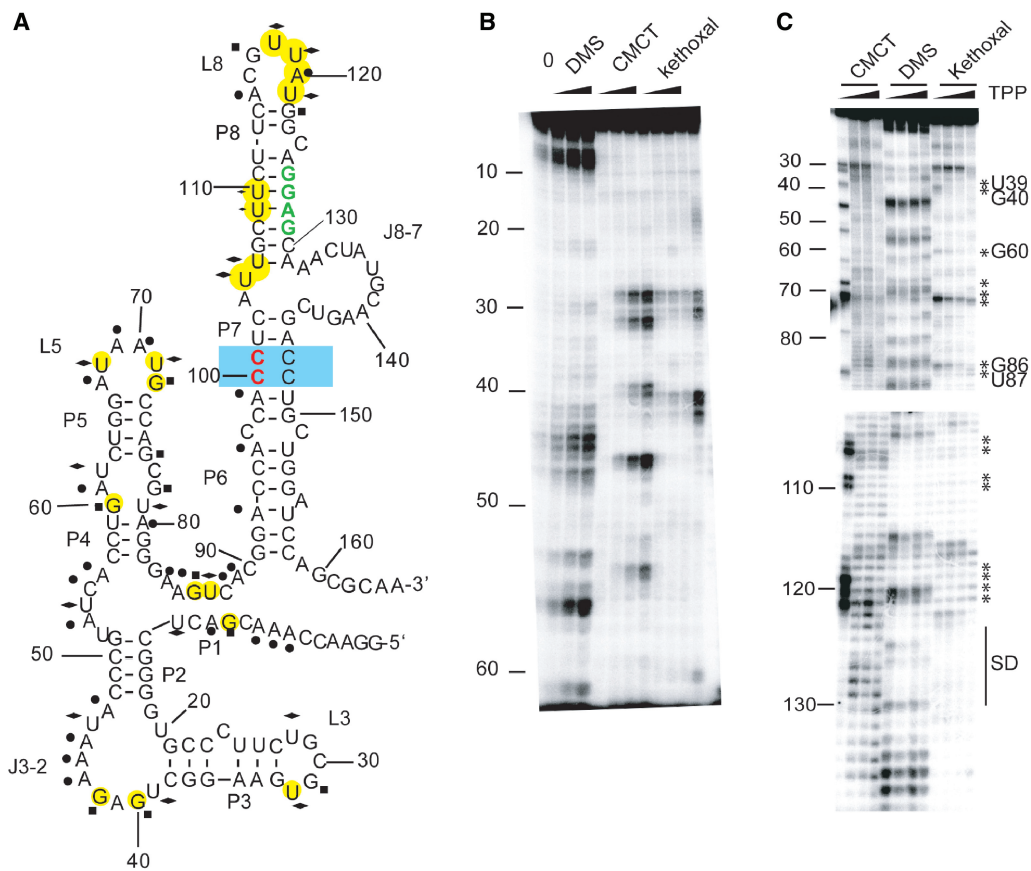


Figure 6. Secondary structure of the TPP-free form of mutant M4 of the thiM riboswitch (A) as well as primer extension reactions after chemical modifications of the riboswitch with CMCT, DMS or kethoxal (B,C). Positions that are chemically modified are marked with symbols (DMS, black dot; kethoxal, black square; CMCT, black diamond). Untreated RNA is referred to as 0. Positions with TPP-induced changes of the chemical modification pattern are highlighted with yellow circles in the secondary structure (closed, decrease; open, increase in signal intensity) and marked by asterisks in the PAA-gel. The mutated nucleotides in M4 (C100 and C101 instead of G100 and G101 in the wild-type) are shown in red and marked in a blue box. The Shine–Dalgarno sequence is depicted in green.

the transition from the TPP-unbound to the metabolite-bound form. Based on previously reported results of our and other groups we derived the secondary structure of the thiM riboswitch of *E. coli* in the absence of TPP and its conformational conversion upon TPP addition (4–7,12). In the sense of communicating domains, portions of the aptamer domain pair with the parts of the expression domain in the absence of TPP. In previous studies, Winkler *et al.* have shown by inline-probing that the thiM riboswitch undergoes structure modulation upon binding of its ligand (4). The authors found many single-stranded positions in the region of nt 39–80 — which is part of the aptamer domain — exhibiting a reduction in spontaneous cleavage in the presence of TPP. Serganov *et al.* conducted enzymatic probing of the thiM riboswitch using the nucleases V1 (helix specific) and T2 (single-strand specific) to further confirm the TPP-binding sites derived from their crystal structure of the aptamer domain of the thiM riboswitch (5). TPP-induced changes in our chemical probings are consistent with TPP-binding sites known from the crystal structure of the aptamer domain observed by Serganov *et al.*

Within the expression domain of the thiM riboswitch Winkler *et al.* observed low spontaneous cleavage by

inline-probing for the proposed stems P2–P7, indicating that the corresponding nucleotides remain structured in both the presence and absence of TPP (4). Consistent with our results, they found that within the expression domain of the thiM riboswitch the region comprising nt 126–130 becomes more structured upon TPP addition (4). The conformational changes observed in our study are more dramatic than suggested by the in-line probing data, and include parts of the aptamer- and the expression-domain. In this manner, our data suggest that the expression domain initially pairs with a large part of the aptamer domain in the absence of TPP. The TPP-induced conformational transition results in a paired anti-SD sequence and renders the ribosome-binding site unpaired, thus allowing translation initiation.

Upon TPP-binding the anti-SD sequence becomes unpaired and sequesters the SD sequence which leads to inhibition of the translation start. This inter-domain communication leads to global changes in the secondary structure of the thiM riboswitch, without significant changes in the ratio of paired versus unpaired regions, i.e. large portions of the riboswitch that are paired in the TPP-free riboswitch remain engaged in pairing in the TPP-bound form. The same is true for most of the

unpaired regions. Enzymatic and chemical probing data in absence and presence of TPP support our secondary structure model.

Our model reveals that the stem regions P2 and P3 of the aptamer domain are preformed in the TPP-free form of the thiM riboswitch from *E. coli*. These regions were shown to build up one of the helices responsible for binding to the HMP moiety of TPP. The crystal structure of the aptamer domain of the riboswitch reveals that this helix is well ordered in the presence of pyrithiamine which shares the HMP moiety with TPP but completely lacks the pyrophosphate group (7). Sudarsan *et al.* showed that pyrithiamine binds to the thiM riboswitch with an affinity comparable to that of thiamine, but orders of magnitude weaker than that of TPP (15). The pyrophosphate moiety of TPP binds to a second helix consisting of P4 and P5. This helix remains disordered in a crystal structure of the aptamer domain in complex with ligands that lack any phosphate (7). The presence of one phosphate group leads to an ordered structure, and the overall structure of the aptamer domain becomes more compact compared with the complex that is formed by thiamine analog pyrithiamine (7). We show that the stems P4 and P5 of the thiM riboswitch are not preformed in the absence of TPP. Instead, our data suggest that they base pair with parts of the expression domain to form a long helix with a terminal hairpin. Upon addition of TPP this structural element is disrupted and the P4, P5 helices are formed. This conformational change also explains why the short riboswitch-binding RNA hairpin N25.1.22 (12) is released upon the addition of TPP, but not by thiamine, suggesting that binding occurs largely via the HMP moiety, in accordance with structural data. However, N25.1.22 is not competed by the addition of thiamine. The formation of stems P4 and P5 is not possible since thiamine lacks the pyrophosphate moiety. Thus, thiamine is able to bind to the thiM riboswitch but does not induce the conformational changes that are necessary to repress gene expression. Taken together, the secondary structure model that we suggested above on the basis of the binding behavior of the RNA hairpin N25.1.22 was confirmed by the more direct evidence resulting from chemical and enzymatic probing data.

We previously reported that a riboswitch variant M4 with mutations loosening stem P7 cannot exert genetic control any more (12). Here we show by chemical probing that, in contrast to the wild-type 165 thiM riboswitch, the mutant M4 adopts a structure similar to the TPP-bound form of the wild-type riboswitch also in the absence of TPP. The expression domain forms a hairpin-like structure containing the stems P6, P8 and P7, which is partially unpaired due to the introduced mutations. Probing data indicate that the SD sequence is paired even in the absence of TPP and that no TPP-induced structural alterations occur within this region. This means that presence or absence of TPP does not affect the accessibility of the SD sequence and hence the initiation of translation. This is exactly what we observed *in vivo* using β -galactosidase fusion constructs (12). Chemical probing thus provides an explanation for the loss of genetic control in M4.

Interestingly, mutation of G100/101 to Cs seems to favor the TPP-bound form in respect to the TPP-free form of the riboswitch although these mutations disrupt two G–C base pairs in either case. It seems that the mutations and subsequent loss of base pairing destabilize the ultimate hairpin in the TPP-free form to such an extent that it cannot form any more and that this renders formation of the entire stem from nt 70–125 in the TPP-free form unfavorable. In contrast, the hairpin-like structure that is adopted by the TPP-bound form of the thiM riboswitch can still form even if there are two mismatches in stem P7. Stem P7 is flanked on either side by G/C rich stems (P6/P8) that contribute to the stability of this structure. Our data thus indicate a finely balanced equilibrium of the two forms of the riboswitch that is necessary for its ability to exert genetic control. Even sequence alterations that, at a first glance, seem to affect both forms to a similar extent can slightly favor one of the structures and cause loss of genetic control.

In conclusion, our data provide insight into the conformational rearrangements and movements that occur in thiM riboswitches when the TPP-concentration in bacteria increases to a certain threshold level, resulting in gene repression by inhibition of translational initiation. The secondary structures and conformational changes introduced here lead to insights that will be important for the functional engineering of riboswitches and for their further exploration as potential drug targets (16–19). Moreover, the knowledge about the structure of riboswitches in the absence of their ligands might allow the design of allosteric switches based on RNA that do not affect translation efficiency, but enable strong regulation by the addition of a ligand. Furthermore, the results indicate that short RNA motifs represent a useful and possibly generally applicable tool for detecting conformational changes in allosteric RNAs on a secondary structure level. Accordingly, phylogenetic analysis might provide insight into the conformational changes of expression domains from other ‘thi’-box containing riboswitches, although sequences of these domains are less well conserved than those of the respective aptamer domains.

SUPPLEMENTARY DATA

Supplementary Data are available at NAR Online.

ACKNOWLEDGEMENTS

This work was supported by grants from the Fonds der Chemischen Industrie, the Deutsche Forschungsgemeinschaft, the Sonderforschungsbereich 624. A.R. thanks the Austrian Academy of Sciences for a grant from the Doctoral Scholarship Program. Funding to pay the Open Access publication charges for this article was provided by the University of Bonn.

Conflict of interest statement. None declared.

REFERENCES

- Winkler, W.C. (2005) Riboswitches and the role of noncoding RNAs in bacterial metabolic control. *Curr. Opin. Chem. Biol.*, **9**, 594–602.
- Tucker, B.J. and Breaker, R.R. (2005) Riboswitches as versatile gene control elements. *Curr. Opin. Struct. Biol.*, **15**, 342–348.
- Rodionov, D.A., Vitreschak, A.G., Mironov, A.A. and Gelfand, M.S. (2002) Comparative genomics of thiamin biosynthesis in prokaryotes. New genes and regulatory mechanisms. *J. Biol. Chem.*, **277**, 48949–48959.
- Winkler, W., Nahvi, A. and Breaker, R.R. (2002) Thiamine derivatives bind messenger RNAs directly to regulate bacterial gene expression. *Nature*, **419**, 952–956.
- Serganov, A., Polonskaia, A., Phan, A.T., Breaker, R.R. and Patel, D.J. (2006) Structural basis for gene regulation by a thiamine pyrophosphate-sensing riboswitch. *Nature*, **441**, 1167–1171.
- Thore, S., Leibundgut, M. and Ban, N. (2006) Structure of the eukaryotic thiamine pyrophosphate riboswitch with its regulatory ligand. *Science*, **312**, 1208–1211.
- Edwards, T.E. and Ferre-D'Amare, A.R. (2006) Crystal structures of the thi-box riboswitch bound to thiamine pyrophosphate analogs reveal adaptive RNA-small molecule recognition. *Structure*, **14**, 1459–1468.
- Noeske, J., Richter, C., Stiral, E., Schwalbe, H. and Wöhnert, J. (2006) Phosphate-group recognition by the aptamer domain of the thiamine pyrophosphate sensing riboswitch. *Chembiochem.*, **7**, 1451–1456.
- Noeske, J., Buck, J., Furtig, B., Nasiri, H.R., Schwalbe, H. and Wöhnert, J. (2007) Interplay of 'induced fit' and preorganization in the ligand induced folding of the aptamer domain of the guanine binding riboswitch. *Nucleic Acids Res.*, **35**, 572–583.
- Schwalbe, H., Buck, J., Furtig, B., Noeske, J. and Wöhnert, J. (2007) Structures of RNA switches: insight into molecular recognition and tertiary structure. *Angew. Chem. Int. Ed. Engl.*, **46**, 1212–1219.
- Montange, R.K. and Batey, R.T. (2006) Structure of the S-adenosylmethionine riboswitch regulatory mRNA element. *Nature*, **441**, 1172–1175.
- Mayer, G., Raddatz, M.S., Grunwald, J.D. and Famulok, M. (2007) RNA Ligands That Distinguish Metabolite-Induced Conformations in the TPP Riboswitch. *Angew. Chem. Int. Ed. Engl.*, **46**, 557–560.
- Beaurain, F., Di Primo, C., Toulme, J.J. and Laguerre, M. (2003) Molecular dynamics reveals the stabilizing role of loop closing residues in kissing interactions: comparison between TAR-TAR* and TAR-aptamer. *Nucleic Acids Res.*, **31**, 4275–4284.
- Darfeuille, F., Reigadas, S., Hansen, J.B., Orum, H., Di Primo, C. and Toulme, J.J. (2006) Aptamers targeted to an RNA hairpin show improved specificity compared to that of complementary oligonucleotides. *Biochemistry*, **45**, 12076–12082.
- Sudarsan, N., Cohen-Chalamish, S., Nakamura, S., Emilsson, G.M. and Breaker, R.R. (2005) Thiamine pyrophosphate riboswitches are targets for the antimicrobial compound pyrithiamine. *Chem. Biol.*, **12**, 1325–1335.
- Blount, K.F. and Breaker, R.R. (2006) Riboswitches as antibacterial drug targets. *Nat. Biotechnol.*, **24**, 1558–1564.
- Blount, K.F., Wang, J.X., Lim, J., Sudarsan, N. and Breaker, R.R. (2007) Antibacterial lysine analogs that target lysine riboswitches. *Nat. Chem. Biol.*, **3**, 44–49.
- Blount, K., Puskarz, I., Penchovsky, R. and Breaker, R. (2006) Development and application of a high-throughput assay for glmS riboswitch activators. *RNA Biol.*, **3**, 77–81.
- Mayer, G. and Famulok, M. (2006) High-throughput-compatible assay for glmS riboswitch metabolite dependence. *Chembiochem.*, **7**, 602–604.
- Rentmeister, A., Bill, A., Wahle, T., Walter, J. and Famulok, M. (2006) RNA aptamers selectively modulate protein recruitment to the cytoplasmic domain of beta-secretase BACE1 in vitro. *RNA.*, **12**, 1650–1660.